Cyclic and Bifurcated Hydrogen Bonds

Ralph C. Kerns and Leland C. Allen*

Contribution from the Department of Chemistry, Princeton University, Princeton, New Jersey 08540. *Received February 6, 1978*

Abstract: Electronic structures for representative sequences of cyclic, $(H_2O)_2$, $(HF)_2$, $(H_2S)_2$, and $(HCl)_2$, and bifurcated, $H_3N{\cdot}H_2O$, $(H_2O)_2$, $HF{\cdot}H_2O$, and $(H_2S)_2$, hydrogen bonds have been determined by ab initio molecular orbital calculations. Wave functions for the linear configurations of $H_2O{\cdot}HF$, $(H_2S)_2$, and $(HCl)_2$ were also determined for reference. An extended search of the potential energy surfaces was carried out including restricted and global optimizations. Geometries, total energies, binding energies, dipole moments, charge transfers, and charge density difference plots are reported. Cyclic and bifurcated configurations correspond to saddle points, not local minima. The charge density difference plots show that the pattern of charge gains and losses around proton donors and around electron donors is qualitatively similar for linear, cyclic, and bifurcated bonds. A quantitatively useful rule is given for determining dimerization energies of the cyclic and bifurcated configurations relative to the linear case. This rule extends a previously published model for linear bonds and states that hydrogen bond energies are proportional to the cosine of the angle measuring hydrogen bond nonlinearity and to the inverse ratio of the heavy-atom separations.

The linear hydrogen bond, A-H···B, has been systematically studied for the hydrides of the second and third rows, but only a few selected systems with restricted geometries have been investigated for cyclic and bifurcated bonds.[1] This is surprising since nonlinear configurations occur frequently in the solid state and very probably in biological systems.[2] In addition, there has been a long-standing debate[3] as to whether the ground states of certain simple dimers, e.g., $(HCl)_2$ and $(H_2O)_2$, are cyclic or linear. Current experimental evidence suggests that for all cases investigated linear hydrogen bonds have the lowest energy.[4] The results reported here support this conclusion and we show by detailed force calculations that asymmetric distortions cause reorientation of the cyclic and bifurcated forms to the linear configuration.

Because of their relatively high symmetry and the additive orientation of monomer dipole moments, the cyclic and bifurcated configurations are the most interesting special cases of nonlinear hydrogen bonds and have received the greatest amount of attention experimentally. Therefore it is important to compare their bonding with that in the corresponding linear systems. One approach is comparison and analysis of charge density difference plots, and these diagrams have been constructed for all of the dimers treated here. This method has been used to help characterize many bonding problems; e.g., Bader et al. determined charge density difference maps for diatomic molecules to investigate covalent bond formation.[5] More recently, Morokuma and others have employed such plots quite effectively in studying normal, linear hydrogen bonds.[6] In the present study we find the distribution of gains and losses in cyclic and bifurcated hydrogen bonds to parallel those in the linear case. Qualitatively, there is a common charge-density pattern around proton donors and around electron donors. Superposition of these common fragments on the appropriate nuclear framework is found to account for the quantum mechanically computed charge density difference plots.

A direct extension of a previously given model for linear hydrogen bonds provides a rule for determining the dimerization energies of cyclic and bifurcated configurations to within ±20%. Thus it is found that these bond strengths are diminished from the linear case by the cosine of the angle measuring hydrogen bond nonlinearity weighted by the inverse ratio of the heavy-atom separations. This rule is rationalized by the analysis of the charge density difference maps.

Methods and Geometries

The configurations and geometrical notation for the hydrogen bonds reported here are (1) for the linear structure

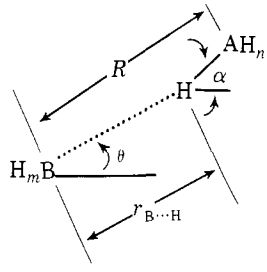

where H_nA = HS and Cl and BH_m = SH_2 and ClH, (2) for the cyclic structure

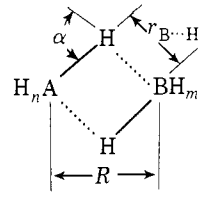

where H_nA = H_mB = HO, F, HS, and Cl, and (3) for the bifurcated structure[7]

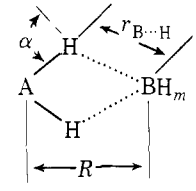

where (A, BH_m) = (O, NH_3), (O, OH_2), (O, FH), and (S, SH_2).

In the above diagrams R is the heavy-atom separation, $r_{B\cdots H}$ the hydrogen bond length, and α the angle of nonlinearity. α is the angle between the vector along the B···H hydrogen bond and the vector along the H-A bond. In its geometry-optimized equilibrium configuration, the hydrogen bond in dimers frequently deviates a few degrees from strict linearity and this equilibrium α is designated α_0. θ, the electron donor angle, is measured between the electron donor symmetry axis and the B···H line.

The wave functions employed were ab initio LCAO-MO-SCF (Roothaan) solutions obtained from the Gaussian 70 computer program.[8] The 4-31G s,p basis set was used throughout.[9] Equilibrium geometries were calculated by the force-relaxation method of Pulay[10] via an especially efficient algorithm written by Schlegel.[11] Two simultaneous conditions for geometry refinement were imposed. (1) The root mean

0002-7863/78/1500-6587$01.00/0 © 1978 American Chemical Society

Table I. Geometries of Monomers

system		r_{AH}, Å	∠HBH, deg	total energy, hartrees	dipole moment, D
		Unassociated Monomers			
NH_3		0.991	115.8	−56.10669[b]	1.420
		(1.012)[a]	(106.7)[a]		(1.47)[c]
H_2O		0.951	111.2	−75.90864[b]	2.487
		(0.957)[d]	(104.5)[d]		(1.85)[c]
HF		0.922		−99.88729[b]	2.287
		(0.917)[e]			(1.82)[c]
H_2S		1.354	95.6	−398.20395[g]	1.775
		(1.328)[f]	(92.2)[f]		(0.97)[c]
HCl		1.299		−459.56342[g]	1.865
		(1.2747)[h]			(1.08)[c]
		Linear			
$HS-H\cdot SH_2$	proton donor		95.7		
	in H bond	1.354			
	external	1.353			
	electron donor	1.353	95.8		
$Cl-H\cdot ClH$	proton donor	1.300			
	electron donor	1.299			
		Cyclic			
$(H_2O)_2$	in H bond	0.953	112.3		
	external	0.949			
$(HF)_2$		0.926			
$(H_2S)_2$	in H-bond	1.353	95.8		
	external	1.353			
$(HCl)_2$		1.299			
		Bifurcated			
$OH_2\cdot NH_3$	proton donor	0.951	107.2		
	electron donor	0.995	113.6		
$(H_2O)_2$	proton donor	0.951	107.1		
	electron donor	0.951	111.5		
$OH_2\cdot FH$	proton donor	0.951	108.7		
	electron donor	0.923			
$(H_2S)_2$	proton donor	1.353	92.2		
	electron donor	1.352	95.9		

[a] K. Kuchitsu, J. P. Guillory, and L. S. Bartell, *J. Chem. Phys.*, **49**, 2488 (1968). [b] W. A. Lathan, W. J. Hehre, L. A. Curtiss, and J. A. Pople, *J. Am. Chem. Soc.*, **93**, 6377 (1971). [c] R. D. Nelson, D. R. Lide, and A. A. Maryott, *Natl. Stand. Ref. Data Ser., Natl. Bur. Stand.*, **No. 10** (1967). [d] W. S. Benedict, N. Gailar, and E. K. Plyler, *J. Chem. Phys.*, **24**, 1139 (1956). [e] G. Herzberg, "The Spectra of Diatomic Molecules", Van Nostrand, Princeton, N.J., 1950. [f] H. C. Allen, Jr., and E. K. Plyler, *J. Chem. Phys.*, **25**, 1132 (1956). [g] J. B. Collins, P. v. R. Schleyer, J. S. Binkley, and J. A. Pople, *J. Chem. Phys.*, **64**, 5142 (1976). [h] E. W. Kaiser, *J. Chem. Phys.*, **53**, 1686 (1970).

square of all of the forces was less than 10^{-3} mdyn for internuclear stretching and 10^{-3} mdyn Å/rad for angle bending. (2) The maximum single force was less than twice the above limits. Typical computation times for a single revised geometry were approximately 1.2 times that required for the MO-SCF computation at that geometry. For each dimer the equilibrium geometries were obtained by complete optimization of all variables subject only to the constraints required to maintain a cyclic or bifurcated configuration. In further calculations these symmetry restrictions were removed to study their reorientation to nearly linear forms.

Results

A. Monomers and Dimers. Table I lists optimized geometries for the monomers, H_3N, H_2O, HF, H_2S, and HCl, both in their unassociated conformation and in the binary complexes. The largest deviations from the unassociated conformation are +0.004 Å in bond length and −4.0° in bond angle. Geometries, energies, and dipole moments for the optimized binary complexes are reported in Table II. Optimized geometries and properties for the linear H_2S and HCl dimers are included here because they have not been obtained previously. Their computed dimerization energies are within the reported experimental range. Although reassuring, this is not a strong claim because experimental values are quite uncertain and many desirable improvements in the wave functions could easily be listed.[12]

The order of decreasing dimerization energy, E_D, for the cyclic systems is $H_2O > HF > HCl > H_2S$ and for the bifurcated systems it is $(H_2O)_2 > H_3N\cdot H_2O > HF\cdot H_2O > (H_2S)_2$. These sequences reproduce the linear dimer E_D order[1] except for the anomalously low $H_3N\cdot H_2O$ value. Unpublished dimerization energy calculations[13] at the 4-31G basis level using experimentally determined monomer geometries in these same complexes plus the bifurcated systems $(H_3N)_2$, $H_2O\cdot H_3N$, and $HF\cdot H_3N$ display the same parallelism with the linear configurations, again with the single exception of $H_3N\cdot H_2O$. Analysis of both data sets reveals the anomaly to lie in a usually large repulsion between the three nitrogen hydrogens and the two oxygen hydrogens due to the particular geometry of the bifurcated configuration and the high strengths of the proton and electron donors. From the collection of all other bifurcated results, an extrapolated E_D value of 6.5 kcal/mol is obtained for $H_3N\cdot H_2O$, implying a not unreasonable value of 1.5 kcal/mol for the extra H-H repulsion energy.

It is known from high-accuracy calculations on linear $(H_2O)_2$ and $(HF)_2$ that for first-row dimers the 4-31G basis overestimates absolute E_D values by 60–70% but that relative magnitudes are well-preserved.[1] Less information is available for second-row dimers, but it appears that E_D values are overestimated by 0–10%, again with relative magnitudes preserved.[1] It has been previously pointed out[1,20] that the 4-31G basis is a somewhat inferior representation for the second row compared to the first. The effect on E_D values is

Table II. Optimum Geometries, Hydrogen Bond Energies, Total Energies, and Dipole Moments

	$r_{B\cdots H}$, Å	α, deg	θ, deg	H-bond energy, kcal/mol	total energy, hartrees	dipole moment, D
Linear						
$HO\text{-}H\cdot OH_2$[a]	1.871	0	32.0	8.22	−151.83038	4.198
$HF\cdot HF$[a]	1.770	10.5	49.4	8.00	−199.78732	4.456
$HS\text{-}H\cdot SH_2$	2.963	0	71.2	1.84	−796.41084	2.320
				(1.7 ± 0.3)[b]		
Cl-H·ClH	2.715	12.8	74.7	2.10		
				(2.14 ± 0.2)[c]	−919.13019	3.121
Cyclic[d]						
	$r_{B\cdots H}$, Å	R_{AB}, Å	α, deg	H-bond energy, kcal/mol	total energy, hartrees	dipole moment, D
$(H_2O)_2$	2.178	2.704	66.4	7.22	−151.82878	0
$(HF)_2$	2.161	2.546	76.1	6.93	−199.78562	0
$(H_2S)_2$	3.345	4.080	66.4	1.32	−796.41000	0
$(HCl)_2$	3.220	3.780	74.5	1.68	−919.12952	0
Bifurcated[e]						
	$r_{B\cdots H}$, Å	R_{AB}, Å	α, deg	H-bond energy, kcal/mol	total energy, hartrees	dipole moment, D
$OH_2\cdot NH_3$	2.721	3.175	70.0	4.96	−132.02323	4.565
$(H_2O)_2$	2.457	2.899	71.7	5.96	−151.82677	5.343
$OH_2\cdot FH$	2.415	2.842	73.0	3.97	−175.80217	5.034
$(H_2S)_2$	3.401	4.163	64.7	1.39	−796.41011	3.822

[a] L. C. Allen, R. C. Kerns, and H. B. Schlegel, submitted to *J. Am. Chem. Soc.* [b] J. E. Lowder, L. A. Kennedy, K. G. P. Sulzman, and S. S. Penner, *J. Quant. Spectrosc. Radiat. Transfer*, **10**, 17 (1970). [c] D. H. Rank, P. Sitaram, W. A. Glickman, and T. A. Wiggins, *J. Chem. Phys.*, **39**, 2673 (1963). [d] Cyclic $(H_2O)_2$ and $(H_2S)_2$ are not planar but have a center of inversion. The external H-A bonds lie symmetrically on opposite sides of the planar H-bond system at an angle with the A-B line of 141.6° for $(H_2O)_2$ and 110.1° for $(H_2S)_2$. [e] $H_3N\cdots H_2O$ consists of a C_{3v} H_3N and a C_{2v} H_2O with the C_3 and C_2 axes coincident.

analogous to use of the STO-3G vs. 4-31G basis in first-row dimers where STO-3G yields dimerization energies in the same range as much more refined bases.

Shown in Chart I are the Mulliken charges for the unassociated monomers. For the binary complexes, the charge *differences* between monomers and the complexes and the magnitudes and directions of electron transfers between monomers are tabulated. One interesting and important observation from these charges is the comparatively small charge transfer in the bifurcated configuration. The average ratio of bifurcated to linear charge transfers is only two-thirds of the average ratio of bifurcated to linear dimerization energies. For the cyclic configuration the net charge transfer is zero by symmetry.[14] Given the charge transfers and nuclear configurations, the overall trends in the Mulliken charges are generally consistent with those to be expected on the basis of dimerization energy ratios with the linear configuration. It may be noted that the charges on cyclic $(HF)_2$ are very similar to those on cyclic $(SH_2)_2$, even though $E_D((HF)_2)$ is 6.93 kcal/mol and $E_D(SH_2)_2)$ is 1.39 kcal/mol. This difference is simply accounted for by the larger internuclear separations in $(SH_2)_2$. Comparing $(HF)_2$ with $(H_2O)_2$ shows that percent changes in E_D, heavy-atom separation, and atomic charges in going from the linear to cyclic configurations are nearly the same for both dimers.

B. Stability of the Cyclic and Bifurcated Configurations. When calculations for the equilibrium geometries of the cyclic $H_3N\cdot H_2O$ and $HF\cdot H_2O$ systems were attempted, it was found that they relaxed to the most stable linear configuration ($H_3N\cdots H\text{-}OH$ and $H_2O\cdots H\text{-}F$,[15] respectively). No stable point on the potential surfaces corresponding to a cyclic system was found. This suggested the possibility that the symmetric systems for which stable cyclic and bifurcated configurations were found might be located on saddle points of the potential surface. This could occur even though a global optimization was carried out because the symmetry assumed at the outset will be maintained throughout since the forces in such a case will also be symmetric yielding symmetric displacements. Therefore, to test for the presence of a saddle point, an asymmetric distortion was introduced into the equilibrium geometries of the bifurcated and cyclic cases. The internal coordinates are

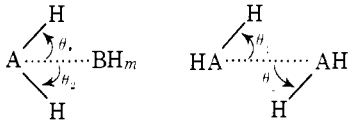

The distortion used was $\delta(\theta_1) = +5°$, $\delta(\theta_2) = -5°$ and calculations were carried out on each system to obtain the resulting forces on θ_1 and θ_2. New internal coordinates ϕ_1 and ϕ_2 were then defined as

$$\phi_1 = (\theta_1 + \theta_2)/2^{1/2}$$

$$\phi_2 = (\theta_1 - \theta_1)/2^{1/2}$$

with the corresponding forces

$$f(\phi_1) = (f(\theta_1) + f(\theta_2))/2^{1/2}$$

$$f(\phi_2) = (f(\theta_1) - f(\theta_2))/2^{1/2}$$

The forces for these new internal coordinates are given in Table III along with the changes in the total energies of the distorted systems relative to the undistorted systems ($\Delta E_t = E_t$(distorted) − E_t(undistorted)). None of the systems studied here shows a cyclic or bifurcated geometry corresponding to a minimum in all directions on its potential surface. Instead, the distorted structures possess forces tending to increase the amount of asymmetric distortion in such a way as to favor a

Chart I

Monomers

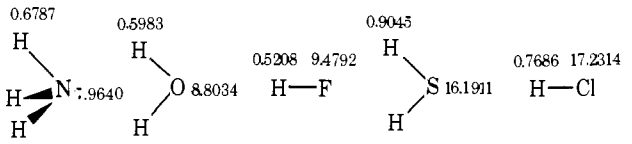

Linear (Difference between Monomer and Complex)

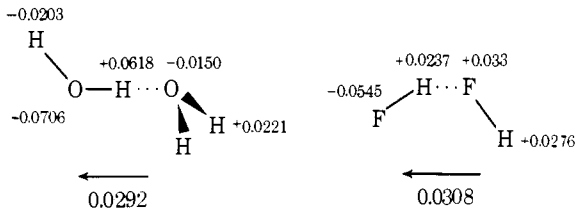

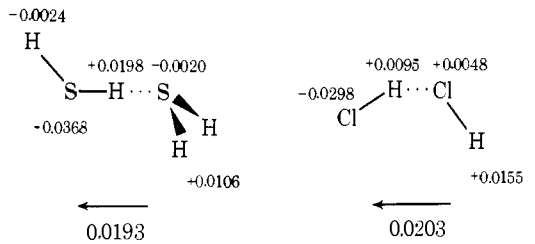

Cyclic (Difference between Monomer and Complex)

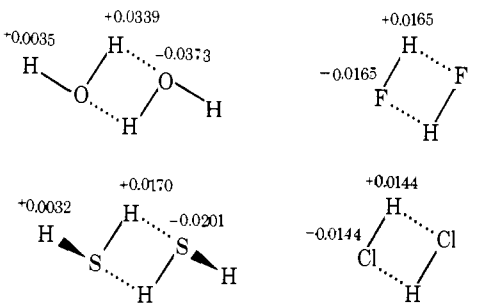

Bifurcated (Difference between Monomer and Complex)

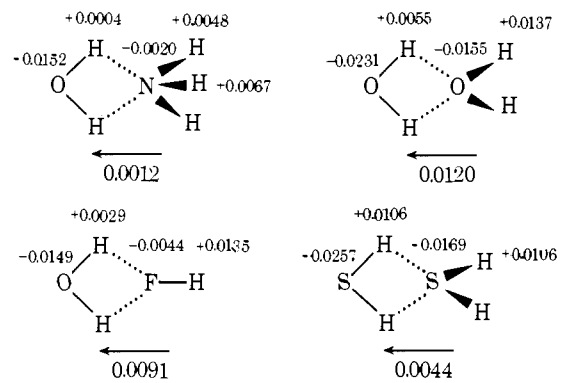

linear H-bonded system. The total energy is lowered by distorting the geometry, again showing that there is no potential minimum at these geometries. For bifurcated $(H_2S)_2$ the potential energy surface is nearly flat and a more complicated distortion than the one employed in generating Table III is required. Thus a 5° in-plane tilt of the electron donor C_2 axis was added to the 5° proton donor C_2 axis rotation and this resulted in electron donor forces implying a further increase in electron donor tilt angles and an energy lowering of ~0.07 kcal/mol. One additional cycle of iteration was carried through

Table III. Forces and Changes in Total Energy Due to an Asymmetric Distortion

system	forces, 10^{-3} mdyn Å/rad $f(\phi_1)$	$f(\phi_2)$	ΔE_T, 10^{-5} hartrees
	Cyclic		
$(H_2O)_2$	1.886	0.965	−1.869
$(HF)_2$	−1.264	2.121	−3.922
$(H_2S)_2$	−0.996	0.485	−1.483
$(HCl)_2$	−0.075	0.825	−1.181
	Bifurcated		
$OH_2{\cdot}NH_3$	0.591	5.728	−8.273
$(H_2O)_2$	1.797	4.471	−6.793
$OH_2{\cdot}FH$	1.462	1.551	−2.552
$(H_2S)_2$	1.704	−1.122[a]	+0.077[a]

[a] See discussion.

(at the same proton donor angle) yielding a still further tilt angle increase and a slightly enhanced distorting force.

C. The Hydrogen Chloride Dimer. A great many experiments have been carried out to determine the structure of the HCl dimer. Far-infrared spectra at first indicated a cyclic dimer,[16] but more recent work using near-infrared and Raman spectra suggest that the hydrogen bond, Cl···H-Cl, is nearly linear with a large electron donor angle[17] (making an L-shaped dimer). Classical force field calculations have been made[18] to simulate the dimer in its solid-state environment and they result in a linear dimer with $2.46 \leq r(\text{Cl}\cdots\text{H}) \leq 2.85$ Å, $\theta \approx 86°$, and $0 \leq \alpha \leq 12°$.

Our fully optimized gas-phase dimer has a geometry in remarkable agreement with these values: $r(\text{Cl}\cdots\text{H}) = 2.72$ Å, $\theta = 74.7°$, and $\alpha_0 = 12.8°$. This linear dimer is 0.42 kcal/mol more stable than the cyclic form. Counterpoise calculations for these two configurations[19] result in a reduction of both E_D values by approximately 1 kcal/mol and an increase in the relative stability of the linear dimer by 12%. Because the monomer dipole moments are almost orthogonal for the equilibrium configuration, Girardet and Robert[18] found from their classical force field calculations that the electrostatic quadrupole-quadrupole interaction is largely responsible for the dimer binding. This is much the same conclusion to be drawn from our quantum mechanical calculations. First, the hydrogen bond is predominantly electrostatic and thus the same multipole interaction argument used by Girardet and Robert applies to our calculations in the limit of no charge redistribution. Second, the charge redistribution effects (which are not included in the classical mechanics calculations) may be assayed from the charge density difference plots. In the section below we show that there exists a characteristic charge density gain-loss distribution around electron donors which possesses a quadrupole-like pattern. The corresponding pattern for proton donors is slightly more elaborate, but looking toward the proton (down the H-A axis), it is apparent that the quadrupole term will be a major component. Thus it is to be expected that charge redistribution results principally in an enhancement of the static quadrupole-quadrupole interaction.

Bonding Pattern and Cos α Rule

A. Charge Density Difference Plots. It is apparent from the $(H_2O)_2$, $(H_2S)_2$, and $(HF)_2$ linear dimers shown at the top of Figures 1, 2, and 3, respectively, and from several previous plots,[6] that there is a characteristic sequence of charge gain, loss, gain, loss, gain, loss, gain, loss as one moves along the bonds from an external point of the proton donor through the dimer to a point external to the electron donor. This gain-loss alternation is a property of the electrostatically driven mutual polarization of the two monomers. Because bonding strength in general falls off as an inverse power of the distance between

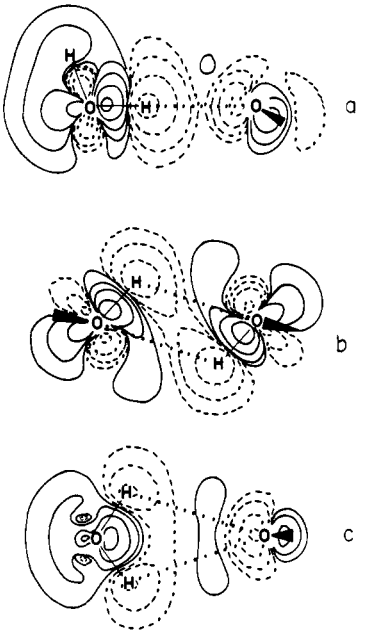

Figure 1. Charge density of water dimer complexes minus charge density of monomers at dimer equilibrium geometries: (a) linear, (b) cyclic, (c) bifurcated. Solid lines indicate charge density gain; dashed lines, loss. Successive contour levels are 0.00032, 0.001, 0.00316, 0.01, 0.0316, and 0.1 e/a_0^3 for both gain and loss.

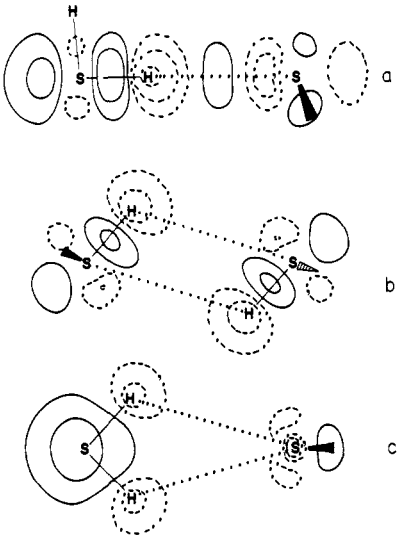

Figure 2. Charge density difference plots for $(H_2S)_2$ at equilibrium geometries: (a) linear, (b) cyclic, (c) bifurcated. Contour levels are as in Figure 1.

positive and negative regions, large charge gains or losses will tend to be concentrated as much as possible on a line connecting the heavy atoms. The off-axis charge gains at the electron donor heavy atom and losses at the proton donor heavy atom result from a slight rehybridization on these atoms which enhances binding by permitting a greater concentration of charge along the line of centers. The principal features of the charge distribution are the charge loss from the electron donor lone pair, the large gain at the proton donor between A and H, and the loss on H. These latter two together constitute an enhancement of the proton donor bond dipole and this is the most prominent characteristic of the charge density difference diagrams.

Turning to the cyclic and bifurcated conformations of $(H_2O)_2$ and $(H_2S)_2$ (Figures 1b,c and 2b,c) and cyclic $(HF)_2$ and $(HCl)_2$ (Figure 3b,c), we observe nearly the same gain-loss sequence as we move from a proton donor external point

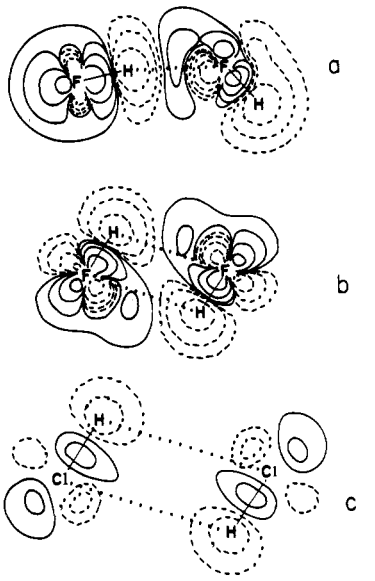

Figure 3. Charge density difference plots at equilibrium geometry of complexes: (a) linear $(HF)_2$, (b) cyclic $(HF)_2$, (c) cyclic $(HCl)_2$. Contour levels are as in Figure 1.

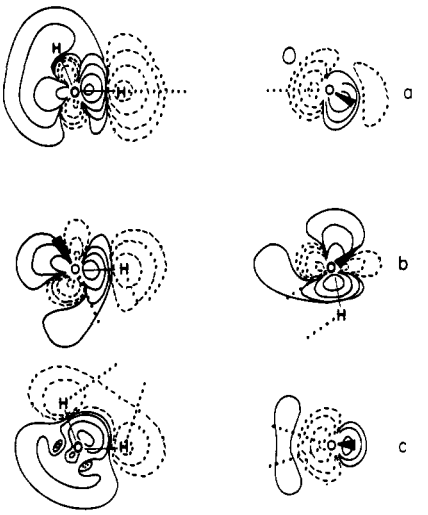

Figure 4. Decomposition and reorientation of water dimer charge density difference plots into proton donor (left side) and electron donor (right side) fragments; (a) linear, (b) cyclic, (c) bifurcated. Proton donor and electron donor fragments are placed at a separation greater than the heavy-atom equilibrium distance for clarity.

along the bent A–H···B path through the electron donor. In particular, the essential features of electron donor lone-pair loss and enhanced proton donor bond dipole are maintained in all cases. Comparison between congeners, $(H_2O)_2$ with $(H_2S)_2$, $(HF)_2$ with $(HCl)_2$, shows that patterns remain the same but magnitudes are reduced because third-row electron donors and proton donors are both weaker than the corresponding second-row donors. These common elements suggest a close similarity with the linear bond. Further support for this hypothesis is obtained by decomposing the dimers into their proton and electron donor fragments and reorienting them. Thus in Figures 4 (H_2O dimers) and 5 (H_2S dimers) the A–H line is chosen as the horizontal axis for proton donors and the symmetry axis of the lone-pair charge loss is also made coincident with the horizontal axis. Along proton donors the detailed charge pattern (left-to-right) is σ-like gain, π-like loss, σ-like gain, σ-like loss. This distribution is a property of the monomer fragment irrespective of the dimer configuration or number of its hydrogen bonds. The similarity in the proton

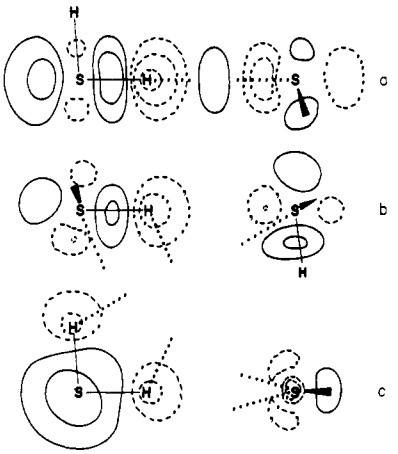

Figure 5. Decomposition and reorientation of charge density difference plots for $(H_2S)_2$ into proton donor (left) and electron donor (right) fragments: (a) linear, (b) cyclic, (c) bifurcated. S- - -S separation is equilibrium value for linear dimer.

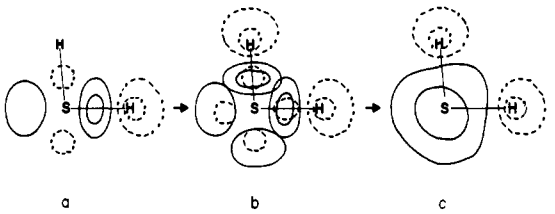

Figure 6. Reconstruction of bifurcated $(H_2S)_2$ proton donor fragment (c) by superposition of two linear proton donor fragments (a). Contours of linear fragment (a) obtained by scaling proton donor in linear dimer according to ratio of E_D values. Gain contours around S in bifurcated $(H_2S)_2$ proton donor (c) are both at +0.00032 level.

donor charge difference pattern between the linear and cyclic configurations is immediately manifest for H_2O and H_2S and this same pattern is clearly visible in cyclic $(HF)_2$ and $(HCl)_2$ (Figure 3b,c) without further decomposition. Proton donors for the bifurcated configuration, however, do not at first appear to be surrounded by the same detailed charge distributions. Figure 6 illustrates the solution to this problem for SH_2 through recognition that the bifurcated geometry implies a double-proton donor. Figure 6a is the proton donor for the linear configuration with contours scaled to the bifurcated E_D. Other features to be noted in Figure 6 are the elliptical charge gain contour around the S atom (Figure 6c) which is at the same level as the outer gain contour, and the cancellation of a −1 (loss) contour against a +2 (gain) contour to yield a +1 contour (Figure 6b) thereby establishing a region at the same level as that already designated by the existing outer contour.

For electron donor heavy atoms, the detailed charge distribution pattern (left-to-right) is σ-like lone-pair loss, π-like gain, σ-like loss. Added to this heavy-atom pattern is a large loss at each hydrogen and a significant gain between hydrogens if there is more than one. For linear $(H_2O)_2$ and $(H_2S)_2$ the lower half of the π-like gain is enhanced by the charge gain between hydrogens. To understand the cyclic configuration, we again take SH_2 as an example and superpose the proton donor of Figure 6a on the basic heavy-atom electron donor pattern with its symmetry axis along the hydrogen bond. If the S-H line were perpendicular to the hydrogen bond line, the gain and loss regions of the proton and electron donors would coincide. Instead, this angle is 66° and the resultant partial overlap of loss and gain regions causes a reduction in contour area and a clockwise rotation of the electron donor symmetry axis due to the large proton donor gain region between S and

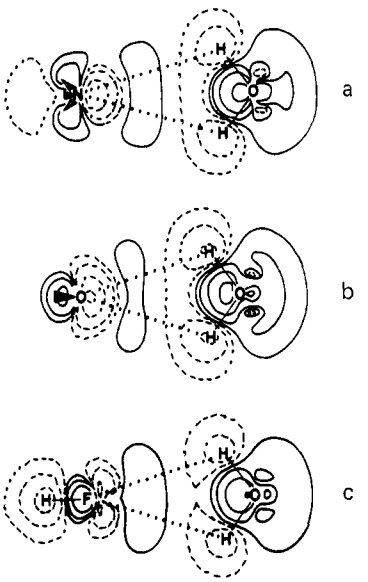

Figure 7. Charge density difference plots for three bifurcated dimers with a common proton donor: (a) $H_3N{\cdot}H_2O$, (b) $H_2O{\cdot}H_2O$, (c) $HF{\cdot}H_2O$. Contour levels are as in Figure 1.

H. The gain between electron donor hydrogens has the same effect and further reduces the right-hand loss region. The lower half of the π-like gain region is augmented because S is also acting as a proton donor.

The electron donor in the bifurcated configuration accommodates two hydrogen bonds separated by a small angle. For $(OH_2)_2$ and $(SH_2)_2$ the addition of two copies of the basic pattern expands the lone-pair loss region sufficiently to eliminate the π-like gains and the gain between hydrogens is larger than the right-hand loss of the heavy-atom pattern. In NH_3 (Figure 7a) the gain between the three hydrogens is greater than that between the two in H_2O and this is sufficient to retain the π-like gain region.

Figure 7 presents three bifurcated dimers having a common proton donor arrayed down the page with their electron donors in the linear hydrogen bond order of decreasing strength. As discussed in the Results section, the same E_D order would obtain for the bifurcated dimers were it not for the extra hydrogen-hydrogen repulsions in $H_3N{\cdot}H_2O$. In spite of this, it is easy to understand the charge density difference consequences of reduced dimerization energy. Proceeding from electron donors H_2O to H_3N to HF, there is a sequential drop in the strength (sum of (contour level)(area) products) of the lone-pair loss regions. Lower strength electron donors polarize the proton donor to a correspondingly lesser extent resulting in the smaller area and fewer contours seen as one goes to lower dimerization energy. This is exactly the same charge density difference plot trend observed for linear dimers. In summary, the bonding in all three hydrogen bond configurations can be described in terms of monomer fragments and, in particular, it is possible to account for the charge redistribution in cyclic and bifurcated configurations using monomer fragments defined by the linear form. Thus the intrinsic nature of the hydrogen bond is the same for all three types. This conclusion is further substantiated by the comparison of dimerization energy ratios given in Table IV. $(H_2O)_2$ is taken as reference for each of the three configurations and the fact that each column shows almost the same set of numbers is indicative of a common bonding mechanism. The only significant deviation occurs for $H_3N{\cdot}H_2O$ and, as before, this anomaly is due to non-hydrogen bond effects.

B. Cos α Rule. Some time ago, a model of the normal, linear hydrogen bond was devised[20] which expressed the dimerization

Table IV. Comparison of Dimerization Energy Ratios in Linear, Cyclic, and Bifurcated Configurations

system	E_D, kcal/mol			$E_D/E_D(H_2O)_2$		
	linear	cyclic	bifurcated	linear	cyclic	bifurcated
$H_3N{\cdot}H_2O$	8.49[a]		4.96	1.03		0.83
$(H_2O)_2$	8.22[a]	7.22	5.96	1.00	1.00	1.00
$HF{\cdot}H_2O$	5.4[b]		3.92	0.66		0.66
$(HF)_2$	8.00[a]	6.93		0.97	0.96	
$H_2S)_2$	1.84	1.32	1.39	0.22	0.19	0.23
$(HCl)_2$	2.10	1.68		0.26	0.23	

[a] L. C. Allen, R. C. Kerns, and H. B. Schlegel, submitted to *J. Amer. Chem. Soc.* [b] J. D. Dill, L. C. Allen, W. C. Topp, and J. A. Pople, *J. Am. Chem. Soc.*, **97**, 7220 (1975).

Table V. Comparison of Cos α Rule and 4-31G Computations

system	α_0, deg	$E_D(\alpha_0)$, kcal/mol	$R(\alpha_0)$, Å	E_D(eq 2), kcal/mol	E_D(MO-SCF), kcal/mol
			Cyclic		
$(H_2O)_2$	0.0[a]	8.22[a]	2.829[a]	6.89	7.22
$(HF)_2$	10.5[a]	8.00[a]	2.687[a]	6.98	6.93
$(H_2S)_2$	0.0	1.84	4.317	1.56	1.32
$(HCl)_2$	12.8	2.10	3.999	2.11	1.68
			Bifurcated		
$OH_2{\cdot}NH_3$	4.3[a]	8.49[a]	2.94[a]	6.47	4.96
$(H_2O)_2$	0.0[a]	8.22[a]	2.829[a]	5.04	5.96
$OH_2{\cdot}FH$	0.0[b]	5.41[b]	2.97[b]	3.31	3.92
$(H_2S)_2$	0.0	1.84	4.317	1.63	1.39

[a] L. C. Allen, R. C. Kerns, and H. B. Schlegel, submitted to *J. Am. Chem. Soc.* [b] J. D. Dill, L. C. Allen, W. C. Topp, and J. A. Pople, *J. Am. Chem. Soc.*, **97**, 7220 (1975).

energy as

$$E_D = K\mu_{A\text{-}H}\Delta I/R$$

where K is a scale factor, $\mu_{A\text{-}H}$ is the bond dipole moment vector along A-H, ΔI is the ionization potential of the hydrogen bonding lone pair referenced to noble-gas atoms, and R is the heavy-atom internuclear separation. For nonlinear hydrogen bonds the deviation from linearity is most simply expressed by the angle α. As shown in the previous section, there exist well-defined charge density difference patterns for electron donors and proton donors which are invariant as to the configuration of the hydrogen bonds. Along A-H the latter pattern consists of large gains at A and losses at H corresponding to an enhancement of the monomer bond dipole moment vector, $\mu_{A\text{-}H}$. $\mu_{A\text{-}H}$ is the driving force for dimer charge redistribution and since the bond between monomers develops along the B···H line, it is only redistribution on this axis which is effective in creating the bond.[21] Thus it is the component of the $\mu_{A\text{-}H}$ vector along B···H which is proportional to dimerization energy, and the linear hydrogen bond formula may be directly extended to the nonlinear case as

$$E_D = K\mu_{A\text{-}H}\cos(\alpha - \alpha_0)\Delta I/R \qquad (1)$$

α_0 measures the small deviation from exact linearity of the equilibrium structure due to non-hydrogen bond forces between the external ligands of A and B. As in the linear configuration, the distance R is the heavy-atom separation because the proton donor center of charge is near A, and the $1/R$ dependence may be considered as the leading term of a multipole expansion.[22] For a specified proton and electron donor the formula may be written compactly as

$$E_D(\alpha) = E_D(\alpha_0)\cos(\alpha - \alpha_0)[R(\alpha_0)/R(\alpha)] \qquad (2)$$

where $E_D(\alpha_0)$ and $R(\alpha_0)$ are the dimerization energy and heavy-atom internuclear separation for the linear (or nearly linear) bond. The above relationship has been verified for small to moderate α.[23] Cyclic and bifurcated configurations, however, correspond to large α values, high symmetry, and favorable alignment of monomer dipole moments, thus providing a severe test of the rule.

Table V compares the predictions of eq 2 with the ab initio calculations and we find that eq 2 is able to order correctly the combined set of cyclic and bifurcated dimers with the exception of $H_3N{\cdot}H_2O$ and the cyclic pair $(H_2O)_2$ and $(HF)_2$. Using the extrapolated $H_3N{\cdot}H_2O$ E_D value (6.5 kcal/mol) corrects the ordering for this dimer and puts its eq 2 prediction in line with the other values. For the cyclic pair, $(H_2O)_2$ and $(HF)_2$, E_D values are so close (0.09 kcal/mol) that they should more appropriately be considered equal and this is reflected in the eq 2 errors of 5 and 1%, respectively. It should also be noted that the fractional change in cos α for specified α is proportional to tan α and therefore a strong function of α for very large α, emphasizing the importance of the fully optimized geometries employed throughout the present study. One particularly satisfying result is the ability of eq 2 to yield reasonable ratios of bifurcated to cyclic E_D values for $(H_2O)_2$ (0.83 ab initio, 0.73 eq 2) and for $(H_2S)_2$ (1.05, 1.02) even though the relative dimerization energy magnitudes are reversed for these two congeners. This result assumes added significance when the Mulliken charges are examined: these clearly imply cyclic E_D > bifurcated E_D for both $(H_2O)_2$ and $(H_2S)_2$. It may also be noted that the origin of the relatively small to vanishing charge transfers associated with the bifurcated and cyclic configurations is traceable to large α.

The existence of invariant proton donor and electron donor charge difference patterns which act as building blocks for constructing the three hydrogen bond configurations and the cos α rule are compatible with recent studies on the origin of hydrogen bonding and help rationalize some of these findings. A variety of experimental and theoretical techniques have shown that normal, linear hydrogen bonds are dominated by electrostatic forces.[24] For linear, cyclic, and bifurcated $(H_2O)_2$ and linear and cyclic $(HF)_2$, Morokuma[25] has applied his energy decomposition analysis to 4-31G MO-SCF wave functions and found all three configurations dominated by the electro-

static component. Moreover, it is losses in the electrostatic component which are principally responsible for the diminished dimerization energy of cyclic and bifurcated configurations.[25] Electrostatic interactions clearly favor a linear hydrogen bond and to a first approximation they vary with α as cos α.

Summary

(1) Wave functions employing the 4-31G s,p basis for a representative selection of linear, cyclic, and bifurcated normal hydrogen-bonded dimers were obtained at their optimum gas-phase geometries by the Pulay force-relaxation method. Cyclic and bifurcated configurations were found to be saddle points, not local minima on the potential surfaces.

(2) The reported calculations strongly support the current experimental belief that normal hydrogen bonds are linear in their minimum-energy configuration. In particular, the long-standing question of the HCl dimer was treated in detail and our results are in close agreement with the classical force field calculations. These indicate that the electrostatic quadrupole–quadrupole interaction dominates the binding.

(3) Dimerization energies and charge density difference plots show common trends between linear, cyclic, and bifurcated configurations. The most prominent charge distribution features in all cases are an electron donor lone-pair loss region, a large gain centered near A between A and H, and a sizable loss on H.

(4) The charge density difference diagrams may be decomposed into characteristic electron donor and proton donor fragments which are invariant as to the number and configuration of the hydrogen bonds. Linear, cyclic, and bifurcated configurations can be constructed using these fragments as building blocks thus demonstrating the common nature of the binding among all of the three types.

(5) A quantitatively useful dimerization energy rule was given:

$$E_D(\alpha) = E_D(\alpha_0)[R(\alpha_0)/R(\alpha)] \cos(\alpha - \alpha_0)$$

Angle α measures the nonlinearity, α_0 is the residual deviation from linearity often present in the linear configuration, and R is the heavy-atom separation. This rule provides a simple formula capable of approximately ±20% accuracy for all normal hydrogen bonds.

(6) The cos α rule and the existence of invariant electron donor and proton donor fragments are compatible with recent work suggesting that electrostatic interactions are the principal binding mechanism in the normal hydrogen bond and with the finding that a reduced electrostatic contribution is responsible for the lower values of E_D in cyclic and bifurcated configurations relative to the linear form.

Acknowledgment. The optimized geometry calculations employed in this work owe their practical realization to the computer program FORCE written by Dr. H. Bernhard Schlegel and we thank him for its use and for numerous helpful discussions. Dr. William C. Topp carried out some of the initial work on $(HCl)_2$ and Linda D. Fredrickson did some of the initial calculations on $(SH_2)_2$ and we thank them for their efforts. Financial support was provided by Grant PCM 76-23236 from the Biophysics Program, Molecular Biology Section of the National Science Foundation, and we are grateful for this assistance.

References and Notes

(1) P. A. Kollman, "Modern Theoretical Chemistry", Vol. 4, H. F. Schaefer, Ed., Plenum Press, New York, N.Y., 1977, Chapter 3; P. Schuster, "The Hydrogen Bond", P. Schuster, G. Zundel, and C. Sandorfy, Eds., North-Holland Publishing Co., Amsterdam, 1976, Chapter 2; W. C. Topp and L. C. Allen, *J. Am. Chem. Soc.*, **96**, 5291 (1974); P. A. Kollman, J. McKelvey, A. Johansson, and S. Rothenberg, *ibid.*, **97**, 955 (1975); J. D. Dill, L. C. Allen, W. C. Topp, and J. A. Pople, *ibid.*, **97**, 7220 (1975); S. Yamabe, S. Kato, H. Fujimoto, and K. Fukui, *Bull. Chem. Soc. Jpn.*, **48**, 1 (1975); P. A. Kollman and L. C. Allen, *J. Chem. Phys.*, **51**, 3286 (1969); K. Morokuma and L. Pedersen, *ibid.*, **48**, 3275 (1968); H. Umeyama and K. Morokuma, *J. Am. Chem. Soc.*, **99**, 1316 (1977); S. N. Vinogradov and R. H. Linnell, "Hydrogen Bonding", Van Nostrand Reinhold, New York, N.Y. 1971.

(2) W. A. P. Luck, "The Hydrogen Bond", P. Schuster, G. Zundel, and C. Sandorfy, Eds., North-Holland Publishing Co., Amsterdam, 1976, Chapter 11; I. Olovsson and P. G. Jönsson, *ibid.*, Chapter 8; A. F. Wells, "Structural Inorganic Chemistry", 4th ed., Clarendon Press, Oxford 1975; D. M. Adams, "Inorganic Solids", Wiley, New York, N.Y., 1974; W. H. Baur, in "Handbook of Geochemistry", Vol. 2, 1-A-1, Springer-Verlag, West Berlin, 1970; R. Chidambaram, *Proc. Nucl. Phys. Solid State Phys. Symp., 13th*, **1**, 215 (1969); R. Balasubramanian, R. Chidambaram, and G. N. Ramachandran, *Biochim. Biophys. Acta*, **221**, 182, 196 (1970).

(3) H. E. Hallam, "The Hydrogen Bond", P. Schuster, G. Zundel, and C. Sandorfy, Eds., North-Holland Publishing Co., Amsterdam, 1976, Chapter 22.

(4) $(H_2O)_2$: P. Saumagne, *J. Chem. Phys.*, **53**, 3768 (1970); G. P. Ayers and A. D. E. Pullin, *Spectrochim. Acta, Part A*, **32a**, 1629, 1641, 1689, 1695 (1976); T. R. Dyke, *J. Chem. Phys.*, **66**, 492 (1977); T. R. Dyke, K. M. Mack, and J. S. Muenter, *ibid.*, 498 (1977); L. Fredin, B. N. Nelander, and G. Ribbegård, *ibid.*, 4065, 4073 (1977). $(HCl)_2$: D. Maillard, J. P. Perchard, and A. Schriver, *Mol. Spectrosc. Dense Phases, Proc. 12th Eur. Cong. Mol. Spectrosc.*, 337 (1976); J. C. Bureau, L. C. Brunel, and M. Peyron, *ibid.*, 369 (1976).

(5) R. F. W. Bader, W. H. Henneker, and P. E. Cade, *J. Chem. Phys.*, **46**, 3341 (1967); R. F. W. Bader, I. Keaveny, and P. E. Cade, *ibid.*, **47**, 3381 (1967).

(6) S. Yamabe and K. Morokuma, *J. Am. Chem. Soc.*, **97**, 4458 (1975); P. A. Kollman and L. C. Allen, *J. Chem. Phys.*, **52**, 5085 (1970); M. Dreyfus, B. Maigret, and A. Pullman, *Theor. Chim. Acta*, **17**, 109 (1970); G. H. F. Diercksen, *ibid.*, **21**, 335 (1971).

(7) This definition of the bifurcated configuration has been used in most theoretical investigations. It is the appropriate one here because it allows direct comparison with linear and cyclic dimers. Baur and Chidambaram[2] give an alternative definition that has two hydrogen bonds emanating from the proton donor. Three hydrogen bonds can also be associated with a single proton donor or a single electron donor and we are currently studying these various configurations.

(8) W. J. Hehre, W. A. Lathan, R. Ditchfield, M. D. Newton, and J. A. Pople, Program 236, Quantum Chemistry Program Exchange, Indiana University, Bloomington, Ind.

(9) R. Ditchfield, W. J. Hehre, and J. A. Pople, *J. Chem. Phys.*, **54**, 724 (1971).

(10) P. Pulay and W. Meyer, *Mol. Phys.*, **27**, 473 (1974); P. Pulay, "Modern Theoretical Chemistry", Vol. 4, H. F. Schaefer, Ed., Plenum Press, New York, N.Y., 1977, Chapter 4.

(11) H. B. Schlegel, Ph.D. Thesis, Queen's University, Kingston, Canada, 1975; H. B. Schlegel, S. Wolfe, and F. Bernardi, *J. Chem. Phys.*, **63**, 3632 (1975).

(12) For the two most important theoretical errors, neglect of zero-point energy and omission of instantaneous electron–electron correlation, there is good evidence that an approximate cancellation occurs: G. F. H. Diercksen, W. P. Kraemer, and B. O. Roos, *Theor. Chim. Acta*, **36**, 249 (1975).

(13) All chemical trends are the same as those for the systems reported here, but the monomer energy changes between theoretical optimum geometries and experimental geometries involve energy differences that are a significant fraction of the dimerization energies; thus these calculations can not be employed to test hypotheses such as the cos α rule.

(14) Although the net charge transfer is zero, this does not imply that the charge-transfer contribution to the dimerization energy is zero. See ref 25 for estimates of this contribution in cyclic $(H_2O)_2$ and $(HF)_2$.

(15) R(O–F) for the fully optimized dimer is 2.61 Å and the computed dipole moment is 5.58 D. Computed values for the dipole moments of both monomers overestimate those from experiment by approximately 31%, thereby leading to a scaled prediction of 4.28 for the H_2O·HF complex. Both R and the scaled dipole moment are sufficiently close to the microwave spectroscopy results, R = 2.68 Å, μ = 3.82 D (J. W. Bevan, A. C. Legon, D. J. Millen, and S. C. Rogers, *J. Chem. Soc., Chem. Commun.*, 341 (1975)), to establish the linear configuration with oxygen as electron donor as the minimum-energy configuration. Cyclic and bifurcated configurations can likewise be rejected.

(16) B. Katz, A. Ron, and O. Schnepp, *J. Chem. Phys.*, **47**, 5303 (1967).

(17) D. Maillard, J. P. Perchard, and A. Schriver, *Mol. Spectrosc. Dense Phases, Proc. 12th Eur. Cong. Mol. Spectrosc.*, 337 (1976); J. C. Bureau, L. C. Brunel, and M. Peyron, *ibid.*, 369 (1976).

(18) C. Girardet and D. Robert, *J. Chem. Phys.*, **59**, 4110, 5020 (1973).

(19) A. Johansson, P. A. Kollman, and S. Rothenberg, *Theor. Chim. Acta*, **29**, 167 (1973), and M. D. Newton and S. Ehrenson, *J. Am. Chem. Soc.*, **93**, 4971 (1971), have applied this technique to hydrogen-bonded systems and the latter authors also find an approximately 1 kcal/mol lowering in their 4-31G MO-SCF study of water polymers. Our $(HCl)_2$ estimate was obtained from calculations carried out by W. C. Topp using the 4-31G basis with experimental monomer geometries.

(20) L. C. Allen, *J. Am. Chem. Soc.*, **97**, 6921 (1975); *Proc. Natl. Acad. Sci.*, **72**, 4701 (1975).

(21) This is analogous to the angular dependence of the scattering cross section in a time-independent formulation.

(22) R in cyclic and bifurcated dimers may be larger or smaller than R in the corresponding linear configuration, but r(H···B) is always larger and is inversely proportional to E_D.

(23) L. C. Allen, R. C. Kerns, and H. B. Schlegel, submitted to *J. Am. Chem. Soc.*

(24) J. F. Griffin and P. Coppens, *J. Am. Chem. Soc.*, **97**, 3496 (1975); R. S. Brown and R. W. Marcinko, *ibid.*, **99**, 6500 (1977); H. Umeyama and K. Morokuma, *ibid.*, 1316 (1977); P. A. Kollman, *ibid.*, 4875 (1977); M. Dreyfus and A. Pullman, *Theor. Chim. Acta*, **19**, 20 (1970); P. A. Kollman and L. C. Allen, *ibid.*, **18**, 399 (1970); S. Yamabe, S. Kato, H. Fujimoto, and K. Fukui, *Bull. Chem. Soc. Jpn.*, **48**, 1 (1975).

(25) H. Umeyama and K. Morokuma, *J. Am. Chem. Soc.*, **99**, 1316 (1977).